nature medicine

Targeting megakaryocytic-induced fibrosis in myeloproliferative neoplasms by AURKA inhibition

Qiang Jeremy Wen[1,7], Qiong Yang[1,7], Benjamin Goldenson[1], Sébastien Malinge[2], Terra Lasho[3], Rebekka K Schneider[4], Lawrence J Breyfogle[4], Rachael Schultz[1], Laure Gilles[1], Priya Koppikar[5], Omar Abdel-Wahab[5], Animesh Pardanani[3], Brady Stein[1], Sandeep Gurbuxani[6], Ann Mullally[4], Ross L Levine[5], Ayalew Tefferi[3] & John D Crispino[1]

Primary myelofibrosis (PMF) is characterized by bone marrow fibrosis, myeloproliferation, extramedullary hematopoiesis, splenomegaly and leukemic progression. Moreover, the bone marrow and spleens of individuals with PMF contain large numbers of atypical megakaryocytes that are postulated to contribute to fibrosis through the release of cytokines, including transforming growth factor (TGF)-β. Although the Janus kinase inhibitor ruxolitinib provides symptomatic relief, it does not reduce the mutant allele burden or substantially reverse fibrosis. Here we show through pharmacologic and genetic studies that aurora kinase A (AURKA) represents a new therapeutic target in PMF. Treatment with MLN8237, a selective AURKA inhibitor, promoted polyploidization and differentiation of megakaryocytes with PMF-associated mutations and had potent antifibrotic and antitumor activity *in vivo* in mouse models of PMF. Moreover, heterozygous deletion of *Aurka* was sufficient to ameliorate fibrosis and other PMF features *in vivo*. Our data suggest that megakaryocytes drive fibrosis in PMF and that targeting them with AURKA inhibitors has the potential to provide therapeutic benefit.

© 2015 Nature America, Inc. All rights reserved.

Although the median survival for individuals with PMF, a subtype of myeloproliferative neoplasms (MPNs), is 5–7 years, those with intermediate and high-risk disease (as defined by the Dynamic International Prognostic Scoring System Plus) have a median survival of just 16–35 months[1]. PMF can develop into acute leukemia and is associated with pancytopenia, thrombosis and cardiac complications, infection and bleeding[2]. Within the bone marrow of individuals with PMF, there are excessive numbers of megakaryocytes with an abnormal nuclear/cytoplasmic ratio and a reduced polyploid state. Experiments using *in vitro* cultures of $CD34^+$ hematopoietic stem cells have shown that megakaryocytes that harbor PMF-associated mutations (hereafter referred to as PMF megakaryocytes) expand excessively, are immature and show delayed apoptosis owing to increased expression of the anti-apoptotic factor Bcl-xL[3]. Mutations associated with PMF include those that affect genes involved in signaling by the Janus kinase (JAK) and signal transducer and activator of transcription (STAT) factors (such as *JAK2* and *MPL*, which encodes the surface receptor for the megakaryocyte growth and differentiation factor thrombopoietin (THPO)), endoplasmic reticulum stress (such as *CALR*, which encodes the Ca^{2+}-binding protein calreticulin), epigenetic regulation (such as *TET2* and *ASXL1*) and RNA splicing (such as *SRSF2* and *SF3B1*)[4–8]. Although ruxolitinib, a JAK inhibitor approved for use in individuals with PMF[9,10], provides symptomatic relief and extends survival, it does not reduce the mutant allele burden or alter the natural history of the disease[2,11,12]. Moreover, many patients are intolerant to ruxolitinib and discontinue therapy because of its side effects, which include anemia and thrombocytopenia[13]. Thus, additional agents that have fewer side effects, reduce fibrosis and decrease the mutant allele burden are needed.

Several lines of evidence suggest that increased numbers of megakaryocytes in the bone marrow contribute to marrow fibrosis. First, mice that overexpress *Thpo*, the gene encoding thrombopoietin, develop fibrosis that is associated with increased megakaryocyte numbers[14]. Second, mice with a megakaryocyte-specific deficiency of the transcription factor–encoding gene *Gata1* show elevated numbers of immature megakaryocytes in the bone marrow and severe fibrosis[15,16]. Third, megakaryocytes from individuals with PMF secrete increased levels of the fibrotic cytokine TGF-β, as compared to megakaryocytes from control individuals[3]. However, the extent to which megakaryocytes are required for myelofibrosis and whether targeting the megakaryocyte lineage is sufficient to treat the disease has not been shown.

We recently reported the identification of small molecules that induce megakaryocyte polyploidization, differentiation and subsequent apoptosis[17]. One of these compounds is the AURKA inhibitor MLN8237 (ref. 18). Because megakaryocytes in PMF show impaired differentiation, we hypothesized that AURKA inhibition would induce megakaryocyte maturation similar to the effect of MLN8237

[1]Division of Hematology and Oncology, Department of Medicine, Northwestern University, Chicago, Illinois, USA. [2]Institut Gustave Roussy, Paris, France. [3]Division of Hematology, Mayo Clinic, Rochester, Minnesota, USA. [4]Division of Hematology, Department of Medicine, Brigham and Women's Hospital, Harvard Medical School, Boston, Massachusetts, USA. [5]Human Oncology and Pathogenesis Program, Memorial Sloan Kettering Cancer Center, New York, New York, USA. [6]Section of Hematopathology, University of Chicago, Chicago, Illinois, USA. [7]These authors contributed equally to this work. Correspondence should be addressed to J.D.C. (j-crispino@northwestern.edu).

Received 7 August; accepted 15 October; published online 16 November 2015; doi:10.1038/nm.3995

on malignant undifferentiated megakaryocytes in acute megakaryocytic leukemia[17], reduce the burden of immature megakaryocytes and ameliorate the characteristics of PMF, including bone marrow fibrosis. Here we find that AURKA activity is strongly elevated in cells that harbor activating mutations in *JAK2*, *MPL* or *CALR*. Moreover, MLN8237 treatment induces the differentiation and polyploidization of PMF megakaryocytes and reduces disease burden in two mouse models of PMF, *Jak2*^{V617F} and *MPL*^{W515L} mice. We also demonstrate that AURKA is a tractable therapeutic target in PMF, as loss of a single *Aurka* allele is sufficient to prevent PMF phenotypes *in vivo*.

RESULTS

Inhibition of AURKA induces differentiation of *JAK2*- or *MPL*-mutated cells

On the basis of our previous studies showing that the AURKA inhibitor MLN8237 promotes the maturation of malignant megakaryocytes, as well as our hypothesis that atypical megakaryocytes contribute directly to myelofibrosis, we investigated the activity of AURKA inhibitors in PMF. First, we assayed the effect of MLN8237 on the human erythroleukemia (HEL) cell line, which is positive for *JAK2*^{V617F} and is responsive to JAK2 inhibition[19]. MLN8237 treatment decreased the levels of the kinase-active, T288-phosphorylated form of AURKA[18] (p-AURKA) but not those of phosphorylated STAT3 (p-STAT3) or STAT5 (p-STAT5), whereas ruxolitinib treatment decreased the levels of p-STAT3 and p-STAT5 but not p-AURKA (**Supplementary Fig. 1a**). MLN8237 potently inhibited cell growth, with an IC_{50} (the half-maximal inhibitory concentration) of 26.5 nM, whereas the IC_{50} for ruxolitinib was 343 nM (**Supplementary Fig. 1b**). MLN8237 treatment induced polyploidization and upregulation of the megakaryocyte cell surface markers CD41 and CD42 (**Supplementary Fig. 1c–e**). By contrast, ruxolitinib treatment did not have these effects on cell differentiation. Similarly, treatment with MLN8237 but not ruxolitinib displayed growth inhibition and megakaryocyte differentiation activity on the G1ME/MPLW515L cell line (**Supplementary Fig. 2**), which lacks the erythromegakaryocytic transcription factor GATA1 and expresses the W515L mutant, activated form of MPL (MPL^{W515L}). This cell line, derived from GATA1-deficient embryonic stem cells, can differentiate into megakaryocytes upon restoration of GATA1 (ref. 20). G1ME cells are relevant to PMF because patients express reduced levels of GATA1 (ref. 21), and mice that lack GATA1 in megakaryocytes develop profound bone marrow fibrosis[16]. Finally, similar effects were observed in SET-2 cells (**Supplementary Fig. 3a–e**), a human megakaryocytic cell line derived from a patient expressing JAK2^{V617F} (ref. 22).

Next, we extracted protein from bone marrow cells of *Jak2*^{V617F} knock-in mice[23] or from mice transplanted with mouse bone marrow cells overexpressing *MPL*^{W515L} or either of two different *CALR*-mutated genes (*CALR* type 1 and *CALR* type 2)[7,8]; we then assayed the phosphorylation status of AURKA, STAT3 and STAT5. As expected, expression of *Jak2*^{V617F}, *MPL*^{W515L} or mutated *CALR* led to increased levels of phosphorylated STAT5 relative to controls (**Fig. 1a** and **Supplementary Fig. 4**). Moreover, expression of these mutant proteins led to a striking upregulation of both phosphorylated and total AURKA levels (**Fig. 1a**, **Supplementary Fig. 4** and data not shown). MLN8237 treatment of primary mouse bone marrow cells expressing *MPL*^{W515L} or *Jak2*^{V617F} for 6 h led to a decrease in the levels of phosphorylated AURKA without affecting the levels of p-STAT3 or p-STAT5 (**Fig. 1b**,**c**). Of note, although treatment of these cells with increasing doses of ruxolitinib led to a decrease in p-STAT3 and p-STAT5 levels, p-AURKA levels were reduced only at 24 h after treatment and only at concentrations of ruxolitinib above 1 μM (**Supplementary Fig. 5**). Together, these results show that total and phosphorylated AURKA levels are upregulated by expression of *Jak2*^{V617F}, *MPL*^{W515L} or the *CALR* mutants, and that MLN8237 and ruxolitinib treatments differentially affect cell signaling. To confirm that p-AURKA levels are indeed elevated in megakaryocytes expressing *MPL*^{W515L}, we cultured *MPL*^{W515L}-expressing bone marrow cells with THPO. As we previously reported[24], the expression of AURKA declines with megakaryocyte maturation, such that very little protein is detected in control cells after 3 d of culture (**Supplementary Fig. 6**). By contrast, megakaryocytes that express *MPL*^{W515L} displayed persistent p-AURKA expression throughout 7 d of culture.

We next assessed the effect of AURKA inhibition on the growth of *MPL*^{W515L}-expressing bone marrow cells. Treatment with MLN8237 significantly increased the expression of CD41 and CD42, the degree of polyploidization and the annexin V staining of megakaryocytes, as compared to vehicle-treated cells (**Fig. 1d–g**). These results are consistent with our previous observations that AURKA inhibition promotes megakaryocyte differentiation and acts to suppress proliferation of the megakaryocytic lineage[17]. Lastly, we transduced mouse bone marrow cells with retroviruses that express wild-type *MPL* (*MPL*^{WT}) or *MPL*^{W515L} and cultured the cells in methylcellulose to derive hematopoietic colonies in the presence of increasing doses of MLN8237. MLN8237 treatment preferentially inhibited the colony-forming unit activity (both colony-forming unit–megakaryocyte (CFU-MK) and colony-forming unit–myeloid (CFU-myeloid), which are measures of progenitor cell numbers and activity) of MPL^{W515L}-expressing cells relative to that of MPL^{WT}-expressing cells, even at doses as high as 1 μM (**Fig. 1h**,**i**). This selective effect is probably because of a greater dependence on AURKA activity of cells with activated JAK-STAT signaling.

Previous studies have reported that AURKA expression is elevated downstream of JAK2^{V617F} and that this effect is mediated by increased c-MYC protein levels[25–27]. Consistent with this model, we observed increased c-MYC protein levels in bone marrow cells expressing either *JAK2*^{V617F} or *MPL*^{W515L} (**Fig. 1a**). To investigate the link between activated JAK-STAT signaling, c-MYC and AURKA, we studied SET-2 cells. c-MYC protein was readily detected in SET-2 cell extracts and its expression was significantly reduced by ruxolitinib at 48 h after treatment (**Supplementary Fig. 3f**,**g**). This reduction coincided with a decrease in levels of both total and phosphorylated AURKA. By contrast, MLN8237 treatment did not affect c-MYC levels, indicating that the inhibitor acts downstream of the JAK-STAT–MYC axis. To confirm that c-MYC is required for elevated AURKA expression, we knocked down *MYC*, the gene encoding c-MYC, with either of two short hairpin RNAs (shRNAs). As predicted, *MYC* knockdown reduced levels of both total and phosphorylated AURKA (**Supplementary Fig. 7a**). This reduction was associated with increased expression of CD41 and CD42 and with increased apoptosis (**Supplementary Fig. 7b–e**). Of note, the increase in phosphatidylinositol-4,5-bisphosphate 3-kinase (PI3K) and protein kinase B (AKT) signaling that was observed in *JAK2*- and *MPL*-mutated cells (**Fig. 1a**) is not responsible for the increase in p-AURKA, as treatment of SET-2 cells with the AKT inhibitor MK-2206 did not change p-AURKA levels (**Supplementary Fig. 8**).

We next investigated whether AURKA is upregulated in patients with PMF, essential thrombocythemia (ET) or polycythemia vera (PV) (**Supplementary Tables 1** and **2**). Western blot analysis revealed that p-AURKA and AURKA levels are elevated both in CD34$^+$ cells from the peripheral blood of patients with PMF, as compared to CD34$^+$ cells from the cord blood of control individuals, and in peripheral blood

© 2015 Nature America, Inc. All rights reserved.

mononuclear cells of individuals with ET or PV, as compared to peripheral blood mononuclear cells from healthy individuals (**Fig. 2a** and **Supplementary Figs. 9** and **10**). We also observed elevated expression of c-MYC in mononuclear cells from individuals with PMF, ET and PV, in line with our data from studies of mouse cells and the SET-2 cell line. Similarly to those studies, treatment of primary CD34$^+$ cells from individuals with PMF using MLN8237 led to suppression of p-AURKA levels but not of JAK-STAT signaling (**Fig. 2b**,**c**). Furthermore, whereas ruxolitinib treatment rapidly reduced p-STAT5 levels, it did not affect p-AURKA levels until prolonged incubation. Together, these results support the model that enhanced JAK-STAT signaling indirectly leads to an increase in p-AURKA levels.

Lastly, we investigated the effects on MLN8237 treatment on CD34$^+$ cells collected from the peripheral blood of patients with PMF (patients 5–14, **Supplementary Table 1**). Treatment with MLN8237 significantly induced the upregulation of CD41 and CD42 levels (**Fig. 2d**,**e**) and the polyploidization of CD41$^+$ cells, without affecting the DNA content of CD41$^-$ cells (**Fig. 2f**). Moreover, consistent with the concept that

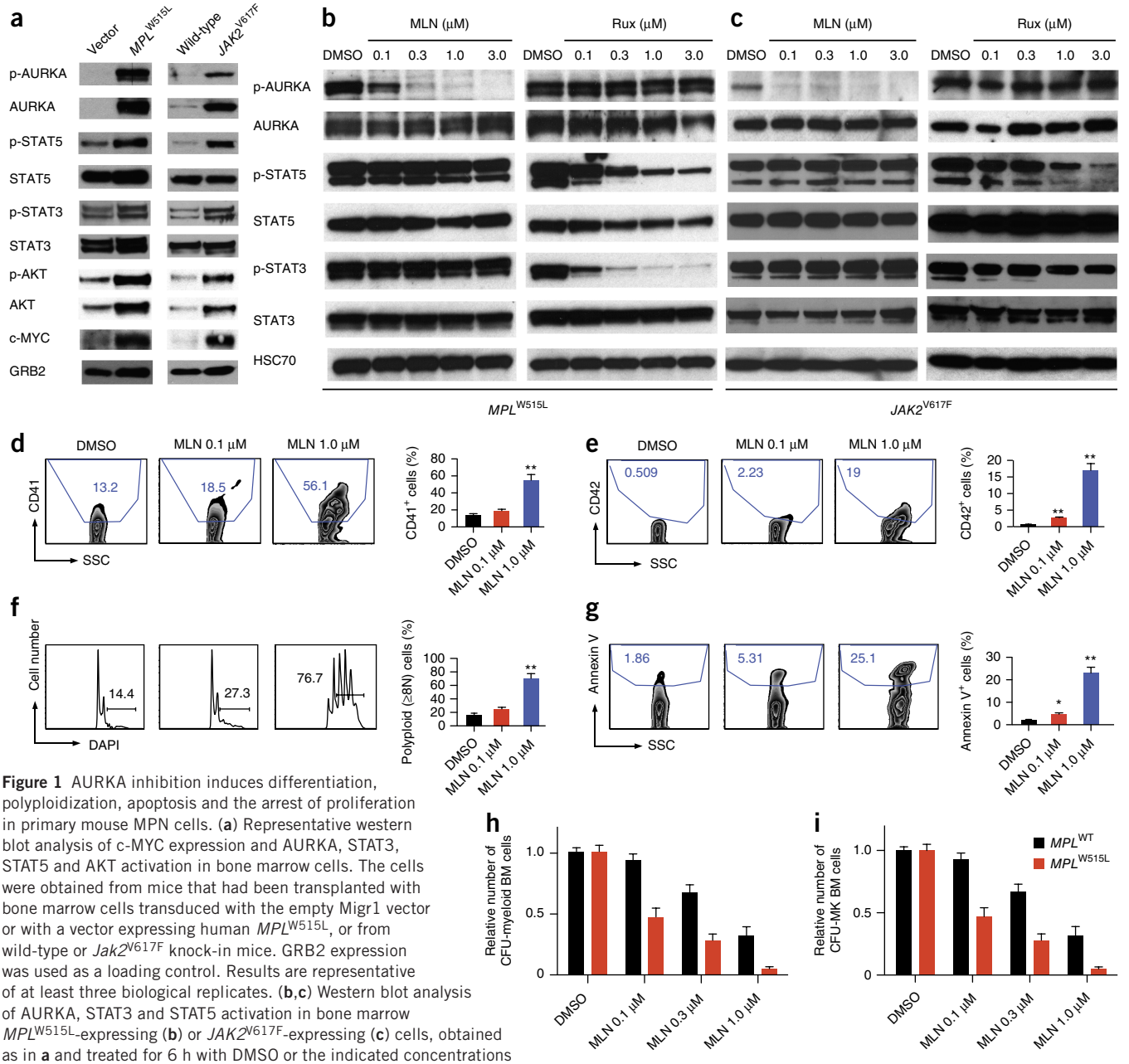

Figure 1 AURKA inhibition induces differentiation, polyploidization, apoptosis and the arrest of proliferation in primary mouse MPN cells. (**a**) Representative western blot analysis of c-MYC expression and AURKA, STAT3, STAT5 and AKT activation in bone marrow cells. The cells were obtained from mice that had been transplanted with bone marrow cells transduced with the empty Migr1 vector or with a vector expressing human *MPL*^{W515L}, or from wild-type or *Jak2*^{V617F} knock-in mice. GRB2 expression was used as a loading control. Results are representative of at least three biological replicates. (**b**,**c**) Western blot analysis of AURKA, STAT3 and STAT5 activation in bone marrow *MPL*^{W515L}-expressing (**b**) or *JAK2*^{V617F}-expressing (**c**) cells, obtained as in **a** and treated for 6 h with DMSO or the indicated concentrations of MLN8237 (MLN) or ruxolitinib (Rux). HSC70 expression was used as a loading control. Results are representative of at least three biological replicates. (**d**–**g**) Flow cytometry plots (left) and quantification (right) of cells showing CD41 (**d**) and CD42 (**e**) expression, polyploidization (i.e., with ≥8N DNA content) (**f**) and apoptosis (**g**) for mouse lineage-negative bone marrow progenitor cells that were transduced with a construct expressing *MPL*^{W515L} and cultured with DMSO or MLN8237 in the presence of THPO for 48 h. Error bars in the graphs represent the mean ± s.d. of two independent experiments conducted in triplicate. $^*P < 0.05$ and $^{**}P < 0.01$, as compared to DMSO treatment; unpaired two-sided Student's *t*-test. SSC, side scatter. DAPI was used to stain DNA. (**h**,**i**) CFU-myeloid and CFU-MK activity of bone marrow (BM) cells expressing *MPL*^{WT} or *MPL*^{W515L} that were treated with DMSO or the indicated concentrations of MLN. The number of colonies was normalized to that observed for DMSO-treated cells. Error bars represent the mean ± s.d. of two independent experiments conducted in duplicate. *MPL*^{W515L} versus *MPL*^{WT}, $P < 0.01$ by two-way analysis of variance (ANOVA).

© 2015 Nature America, Inc. All rights reserved.

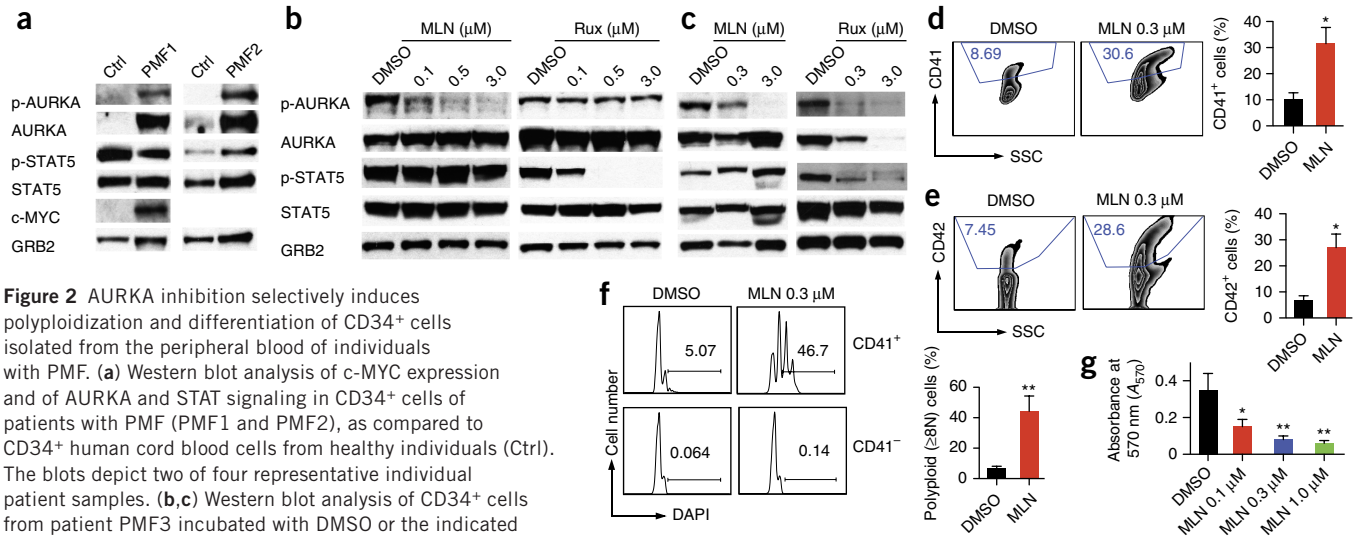

Figure 2 AURKA inhibition selectively induces polyploidization and differentiation of CD34+ cells isolated from the peripheral blood of individuals with PMF. (**a**) Western blot analysis of c-MYC expression and of AURKA and STAT signaling in CD34+ cells of patients with PMF (PMF1 and PMF2), as compared to CD34+ human cord blood cells from healthy individuals (Ctrl). The blots depict two of four representative individual patient samples. (**b**,**c**) Western blot analysis of CD34+ cells from patient PMF3 incubated with DMSO or the indicated concentrations of MLN8237 or ruxolitinib for 6 h (**b**) or 48 h (**c**). Results are representative of two individuals. (**d**–**f**) Flow cytometry plots (left) and quantification (right) of cells showing CD41 expression (**d**), CD42 (**e**) expression and polyploidization (**f**) in CD34+ cells from the peripheral blood of patients with PMF (patients PMF5–PMF14) that were cultured in the presence of DMSO or the indicated concentrations of MLN8237 for 5 d in the presence of THPO. (**g**) Quantification of cells (from **d**–**f**) showing proliferation arrest, as assessed by the Promega CellTiter proliferation assay. Results in **d**–**g** are representative of ten specimens. Error bars represent mean ± s.d.; $*P < 0.05$ and $**P < 0.01$, as compared to DMSO treatment; unpaired two-sided Student's *t*-test.

AURKA inhibition leads to suppression of the megakaryocyte lineage, MLN8237 treatment also inhibited cell growth (**Fig. 2g**).

AURKA inhibitors provide therapeutic benefit in MPN animal models

Before testing MLN8237 in mouse models of MPN, we treated healthy BALB/c mice with MLN8237 (15 mg per kg of body weight (mg/kg)) twice daily for 3 weeks. Our previous pharmacokinetic studies[17] showed that a single dose of 15 mg/kg in mice exceeds the IC_{50} for growth inhibition in *MPL*^{W515L}-expressing primary bone marrow cells for >12 h. MLN8237 treatment of BALB/c mice was well tolerated, with no reduction in body weight or peripheral blood cell counts, and no effect on bone marrow composition (**Supplementary Fig. 11**). Histological analysis of the bone marrow, spleen and liver confirmed

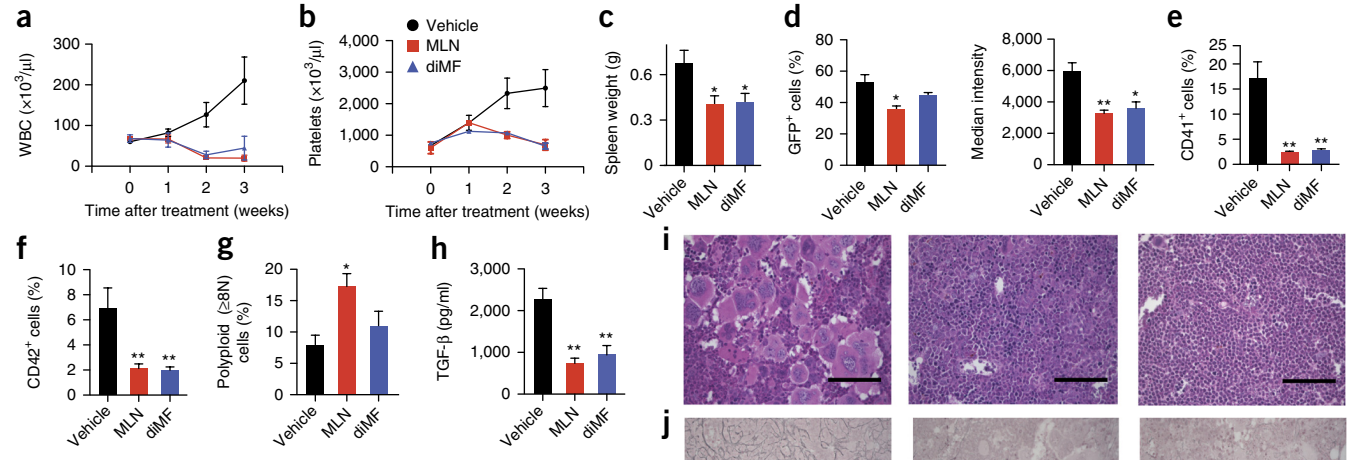

Figure 3 Inhibition of AURKA significantly reduces disease burden in the *MPL*^{W515L} mouse model of myelofibrosis. *MPL*^{W515L} bone marrow–recipient mice were treated with vehicle (15 mg/ml arginine), 15 mg/kg MLN8237 (MLN) or 60 mg/kg diMF (diMF) and were examined for 3 weeks after treatment. (**a**,**b**) White blood cell (WBC, **a**) and platelet (**b**) counts. MLN8237 treatment versus vehicle and diMF treatment versus vehicle were compared and showed $P < 0.01$ by two-way ANOVA. (**c**) Spleen weights of treated mice. (**d**) Percentage of GFP+ cells (left) and the median intensity of GFP staining (right) in the spleens of treated mice. (**e**,**f**) The percentages of CD41+ (**e**) and CD42+ (**f**) cells in the spleen. (**g**) Relative percentages of polyploid megakaryocytes in the spleen, as assessed by staining with a CD41-specific antibody and DAPI. (**h**) Plasma TGF-β levels. (**i**,**j**) Representative images of H&E-stained (**i**) or reticulin-stained (**j**) sections of bone marrow from vehicle-treated (left), MLN8237-treated (middle) or diMF-treated (right) mice. Scale bars, 50 μm. Throughout, results are representative of two independent experiments ($n = 6$ animals per group). Error bars represent mean ± s.d.; $*P < 0.05$ and $**P < 0.01$, as compared to vehicle; unpaired two-sided Student's *t*-test.

© 2015 Nature America, Inc. All rights reserved.

that MLN8237 treatment at this dose did not cause myelosuppression or other detrimental effects (**Supplementary Fig. 11**).

Transplantation of GFP+ bone marrow cells expressing *MPL*^{W515L} leads to an aggressive form of MPN in recipient animals that is characterized by marked leukocytosis, thrombocytosis, hepatomegaly and splenomegaly and the presence of abnormal megakaryocytes and bone marrow fibrosis[28,29]. Three weeks after transplantation of the *MPL*^{W515L}-expressing bone marrow to irradiated BALB/c recipient mice, we verified that all of the animals had >50% GFP+ cells in the peripheral blood (data not shown). At this time point, the animals displayed an elevated white cell count (**Fig. 3a**), indicative of disease. After randomizing the mice, we treated them twice daily for 3 weeks with 15 mg/kg MLN8237, 60 mg/kg of the AURKA inhibitor dimethylfasudil (diMF)[17] or vehicle. As expected, vehicle-treated mice developed an aggressive PMF syndrome that worsened with time[28,29] (**Fig. 3**). By contrast, treatment with either of the AURKA inhibitors normalized white cell and platelet counts, and also reduced the hematocrit and hemoglobin concentrations (**Fig. 3a**,**b** and **Supplementary Fig. 12a**); hemoglobin concentrations are only modestly elevated in this model. Moreover, MLN8237 or diMF treatment reduced spleen and liver weights without affecting body weight (**Fig. 3c** and data not shown). Treatment with either drug also reduced the size of the GFP+ tumor cell population, as assessed by decreases in both the percentage of GFP+ cells and in the median GFP fluorescence intensity (**Fig. 3d**). Consistent with the notion that MLN8237 and diMF act as suppressors of the megakaryocyte lineage, we observed dramatic reductions in the sizes of the CD41 and CD42 populations in the spleen as well as an increased degree of megakaryocyte polyploidization (**Fig. 3e–g**). MLN8237 and diMF treatments had effects on bone marrow megakaryocytes similar to those observed in the spleen (**Supplementary Fig. 12b**,**c**). Treatment with either drug also reduced the splenic Gr1+Mac1+ myeloid cell population and the LSK stem cell and myeloid progenitor populations in the bone marrow (**Supplementary Fig. 12d**,**e** and data not shown). Notably, consistent with a previous report that PMF megakaryocytes secrete excessive amounts of TGF-β (ref. 3), we observed a significant reduction in TGF-β levels in the plasma of animals after MLN8237 or diMF treatment (**Fig. 3h**). Bone marrow histology revealed a robust drop in megakaryocyte mass, accompanied by a striking decline in fibrosis in animals that had been treated with either MLN8237 or diMF (**Fig. 3i**,**j**). We also observed decreased tumor burden in the peripheral blood, spleen, lung and liver (**Supplementary Fig. 12f–i**), as well as decreased fibrosis in the spleen (**Supplementary Fig. 12j**). Finally, we repeated this study in mice with a more fulminant disease by waiting 30 d after transplantation before treating the mice with drugs. In this setting, MLN8237 treatment rapidly normalized peripheral blood counts and decreased splenomegaly, hepatomegaly and megakaryocyte burden (**Supplementary Fig. 13a–e**). This was accompanied by normalization of peripheral blood cytomorphology and of bone marrow, spleen, lung and liver histology, along with variable reduction in bone marrow fibrosis (**Supplementary Fig. 13f–j** and data not shown).

We next studied the activity of MLN8237 treatment in *Jak2*^{V617F} knock-in mice[23]. In this model, recipient mice are transplanted with bone marrow cells from mice with a *loxP*-flanked ('floxed') *Jak2*^{V617F} allele that allows for *Vav-Cre*–mediated expression of JAK2^{V617F}; these animals develop polycythemia, mild leukocytosis, perturbed megakaryopoiesis, splenomegaly, hepatomegaly and myelofibrosis. Four weeks after bone marrow transplantation, we observed polycythemia, leukocytosis and thrombocytosis in the recipient mice. We then treated the animals with 15 mg/kg MLN8237 by oral gavage twice daily for 7 weeks. MLN8237 treatment significantly reduced white blood counts, hematocrit, platelet counts and spleen weight, without affecting body weight (**Fig. 4a**,**b** and data not shown). MLN8237 treatment both reduced the number of erythroid cells and megakaryocytes and induced megakaryocyte polyploidy within the bone marrow and spleen (**Fig. 4c–g**). Moreover, MLN8237

© 2015 Nature America, Inc. All rights reserved.

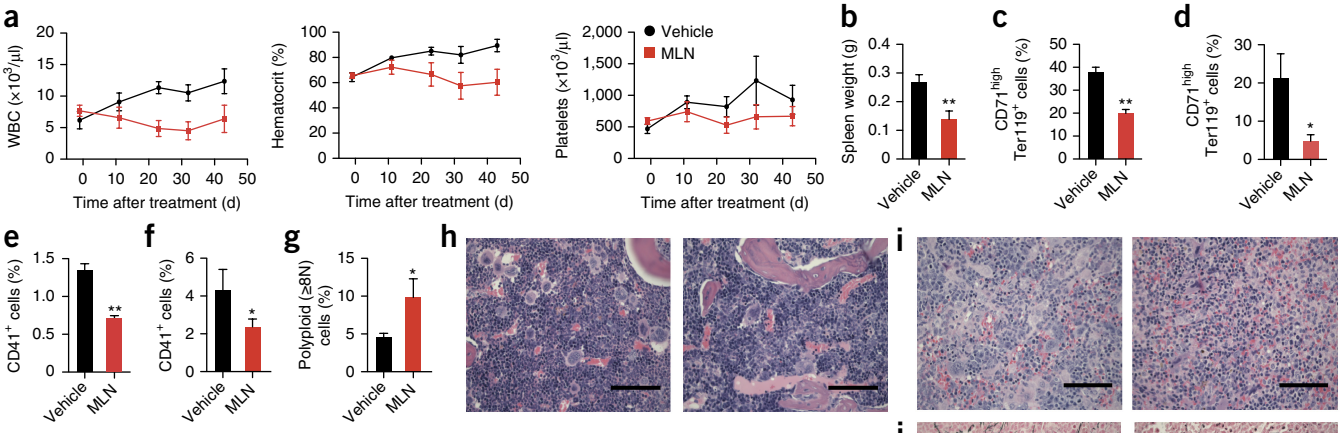

Figure 4 MLN8237 treatment reduces the disease burden of *Jak2*^{V617F}-induced MPN *in vivo*. Transplant recipients of *Jak2*^{V617F}-expressing bone marrow cells were treated with vehicle or 15 mg/kg MLN8237, and were examined after 7 weeks of treatment. (**a**) WBC (left), hematocrit (middle) and platelet (right) counts. $P < 0.01$, MLN8237-treated versus vehicle-treated; two-way ANOVA. (**b**) Spleen weight. (**c–g**) The percentages of CD71^{high}Ter119+ erythroid cells (**c**,**d**) and megakaryocytes (**e**,**f**) in the bone marrow (**c**,**e**) and spleen (**d**,**f**), and the percentage of polyploid (with ≥8N DNA content) CD41+ bone marrow megakaryocytes (**g**), as measured by flow cytometry. (**h**,**i**) H&E-stained sections of bone marrow (**h**) and spleen (**i**) from vehicle-treated (left) or MLN8237-treated (right) mice. (**j**) Reticulin staining of bone marrow sections from vehicle-treated (left) or MLN8237-treated (right) mice. Throughout, results are representative of two experiments ($n = 7$ animals per group). Error bars represent mean ± s.d. Unless specified otherwise, $^{*}P < 0.05$ and $^{**}P < 0.01$, as compared to vehicle; unpaired two-sided Student's *t*-test. Scale bars, 50 μm.

treatment normalized bone marrow megakaryopoiesis and splenic architecture (**Fig. 4h**,**i**) and strikingly attenuated fibrosis in the bone marrow (**Fig. 4j**).

AURKA is required for myelofibrosis

Complete loss of *Aurka* results in early embryonic lethality in mice as a consequence of impaired centrosome separation and defects in bipolar spindle formation, whereas mice with a heterozygous deficiency are viable, fertile and show no hematopoietic defects[24,30]. To determine the requirement for AURKA expression in the development of myelofibrosis, we crossed mice heterozygous for a floxed *Aurka* allele with mice expressing *Mx1-Cre*, which allows for inducible activation of *Cre* in hematopoietic cells, generating *Aurka*$^{fl/+}$ and *Aurka*$^{fl/+}$*Mx1-Cre* mice. Next, we transduced bone marrow cells from these mice with a retrovirus expressing *MPL*^{W515L} and transplanted the cells into lethally irradiated WT recipients. We observed equivalent levels of engraftment of *Aurka*$^{fl/+}$ and *Aurka*$^{fl/+}$*Mx1-Cre* cells at 3 weeks after transplantation, as assessed by the levels of GFP$^+$ cells (**Fig. 5a**). At this time point, we injected *Aurka*$^{fl/+}$ and *Aurka*$^{fl/+}$*Mx1-Cre* mice with polyinosinic-polycytidylic acid (pIpC) to activate the *Mx1* promoter and cause expression of Cre recombinase, which resulted in complete excision of the floxed *Aurka* allele in the cells of the peripheral blood, bone marrow and spleen in mice expressing *Mx1-Cre* (**Fig. 5b**). After the pIpC injection, we observed progression of leukocytosis and thrombocytosis in the control group (i.e., the *Aurka*$^{fl/+}$ mice), but not in the group that was deleted for the floxed *Aurka* allele (i.e., the *Aurka*$^{fl/+}$*Mx1-Cre* mice) (**Fig. 5c**,**d**). In contrast to expansion of the GFP$^+$ tumor population in the control group, tumor cells with heterozygous *Aurka* excision failed to expand (**Fig. 5a**). Heterozygous loss of *Aurka* also led to significant reductions in spleen and liver weights, as well as decreased GFP expression in the spleen (**Fig. 5e**,**f** and **Supplementary Fig. 14a**). In addition, heterozygous loss of *Aurka* led to decreased percentages of splenic CD41$^+$ and Gr1$^+$Mac1$^+$ cells but to an increase in the degree of megakaryocyte polyploidization (**Fig. 5g**,**h** and **Supplementary Fig. 14b**). Finally, heterozygous *Aurka* deletion decreased tumor burden in the peripheral blood, bone marrow, spleen, lung and liver, and also decreased the degree of bone marrow fibrosis (**Fig. 5i**,**j** and **Supplementary Fig. 14c–f**). As expected from our previously published data that mice with complete loss of *Aurka* develop rapid bone marrow failure[24], loss of both alleles of *Aurka* also led to resolution of disease, nearly eliminating the GFP$^+$ tumor cell population (**Supplementary Fig. 15**). Together, these results show that the full gene dosage of *Aurka* is required for the initiation and/or progression of MPN in the *MPL*^{W515L} model, confirming that AURKA is a valid therapeutic target.

MLN8237 synergizes with ruxolitinib *in vitro* and *in vivo*

To determine whether AURKA inhibition can increase the effectiveness of ruxolitinib treatment, we analyzed the effects of combination therapy. Because MLN8237 targets the AURKA pathway and ruxolitinib has a primary effect on the JAK-STAT pathway, we predicted that treatment with these two compounds together would have synergistic effects. We determined the IC_{50} values of MLN8237 and ruxolitinib on CFU-myeloid formation by bone marrow cells of *MPL*^{W515L} bone marrow–recipient mice. Individually, MLN8237 and ruxolitinib treatments had similar effects, with IC_{50} values of 19.4 nM and 22.7 nM, respectively (**Fig. 6a**); however, treatment with combinations of MLN8237 and ruxolitinib inhibited colony formation to a much greater degree than did treatment with either single agent and showed synergy at multiple doses (**Supplementary Table 3**).

Next, we evaluated the activity of combination therapy *in vivo*. Three weeks after engraftment of *MPL*^{W515L}-expressing bone marrow cells in WT recipient mice, we treated animals with submaximal

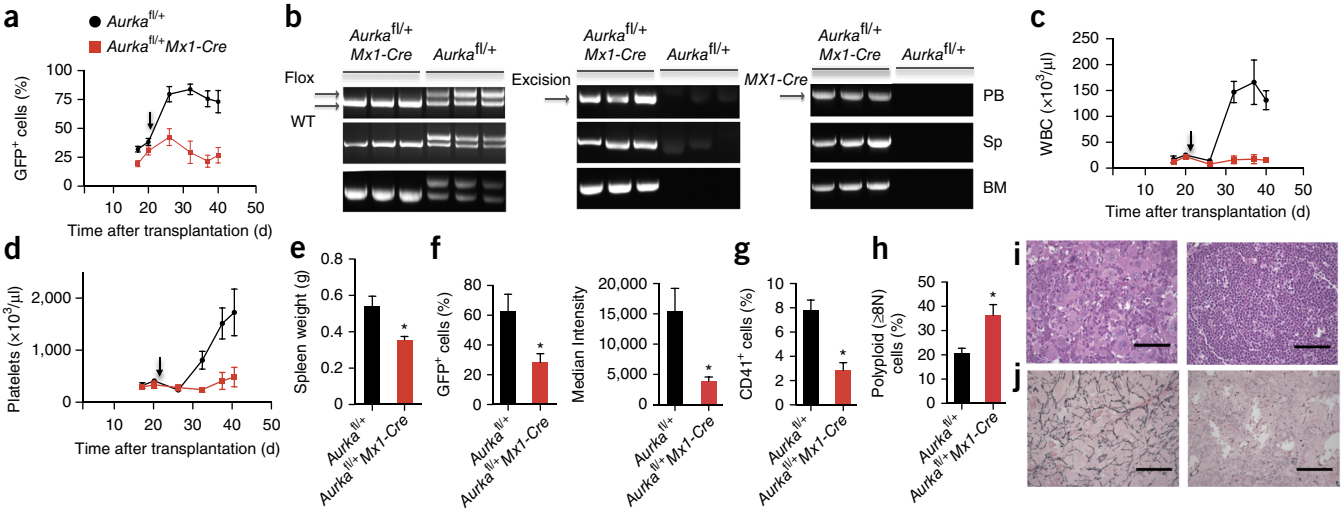

Figure 5 Heterozygous deletion of *Aurka* is sufficient to reduce disease burden in the *MPL*^{W515L} mouse model of myelofibrosis. (**a**) Percentage of GFP$^+$ cells in the peripheral blood of recipient animals that were transplanted with *MPL*^{W515L}-expressing bone marrow from *Aurka*$^{fl/+}$ or *Aurka*$^{fl/+}$*Mx1-Cre* mice and treated with pIpC (indicated by the arrow). (**b**) PCR detection of the floxed (Flox) and WT *Aurka* alleles, the floxed allele after excision (Excision) and the *Mx1-Cre* allele in peripheral blood (PB), spleen (Sp) and bone marrow (BM) of recipient mice 19 d after the first injection of pIpC. (**c**,**d**) WBC (**c**) and platelet (**d**) counts of mice in **a**. In **a**,**c**,**d**, error bars represent mean ± s.d.; $P < 0.01$, *Aurka*$^{fl/+}$ versus *Aurka*$^{fl/+}$*Mx1-Cre*; two-way ANOVA. (**e**) Spleen weights 42 d after transplantation. (**f**–**h**) GFP$^+$ tumor burden (**f**), CD41$^+$ megakaryocytes (**g**) and DNA content of splenic megakaryocytes (**h**) in mice with the indicated genotypes, as determined by flow cytometry 42 d after transplantation. (**i**,**j**) Bone marrow sections from *Aurka*$^{fl/+}$ (left) or *Aurka*$^{fl/+}$*Mx1-Cre* (right) mice stained with H&E (**i**) or for reticulin (**j**) 42 d after transplantation. Scale bars, 50 μm. Throughout, results are representative of two independent experiments (n = 5 animals per group). Unless otherwise stated, error bars represent mean ± s.d.; $^*P < 0.05$, as compared to *Aurka*$^{fl/+}$; unpaired two-sided Student's t-test.

© 2015 Nature America, Inc. All rights reserved.

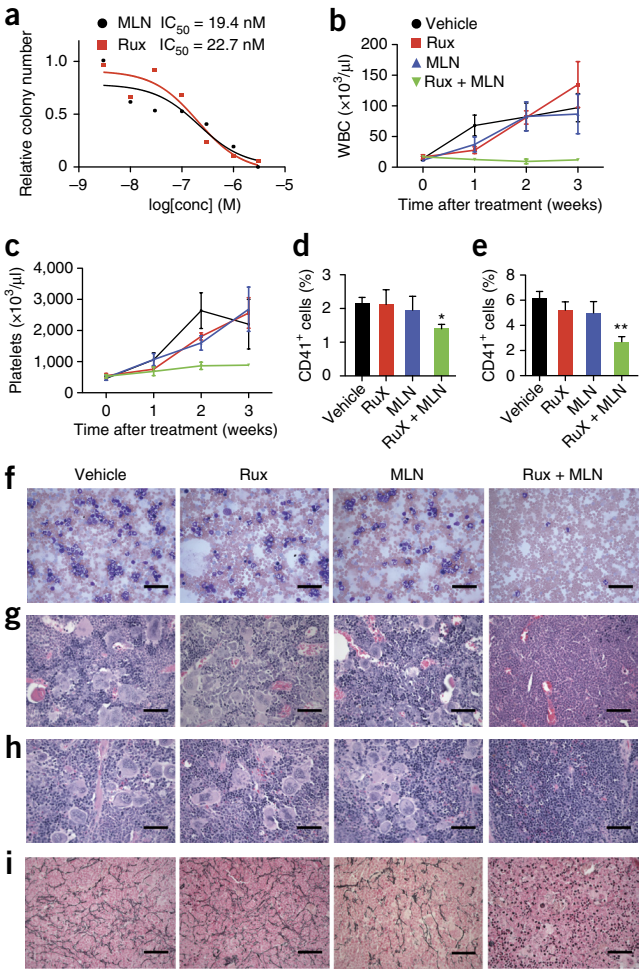

Figure 6 MLN8237 and ruxolitinib act synergistically both *in vitro* and *in vivo*. (**a**) Determination of IC_{50} values for the effects of MLN8237 (MLN) and ruxolitinib (Rux) on myeloid colony formation of bone marrow cells from mice transplanted with *MPL*^{W515L}-expressing cells. (**b**,**c**) WBC (**b**) and platelet (**c**) counts of *MPL*^{W515L} bone marrow–recipient mice treated with submaximal doses of MLN8237 (5 mg/kg) or ruxolitinib (30 mg/kg), or their combination at these doses. MLN + Rux versus vehicle, $P < 0.01$; Rux versus vehicle or MLN versus vehicle, $P < 0.05$; two-way ANOVA. (**d**,**e**) The percentage of CD41$^+$ megakaryocytes in the bone marrow (**d**) and spleen (**e**) 3 weeks after the start of therapy. (**f**–**i**) May-Grunwald Giemsa–stained blood smears (**f**), H&E-stained sections of the bone marrow (**g**) and spleen (**h**), and reticulin staining of bone marrow sections (**i**) 3 weeks after the start of therapy of mice treated with vehicle (left), ruxolitinib (second from left), MLN8237 (second from right), or MLN8237 and ruxolitinib (right). Scale bars, 50 μm. Results are representative of two independent experiments ($n = 5$ animals per group). Error bars represent mean ± s.d.; $^*P < 0.05$ and $^{**}P < 0.01$, as compared to vehicle-treated; one-way ANOVA.

doses of MLN8237 and ruxolitinib, either as single agents or in combination. Whereas treatment with either single agent at these doses did not alter disease progression, treatment with the combination of the drugs led to marked reductions in both white blood cell counts and platelet counts (**Fig. 6b**,**c**), and to significant decreases in megakaryocyte burden within the bone marrow and spleen (**Fig. 6d**,**e**). The efficacy of this combination was further confirmed by major reductions in tumor burden in the peripheral blood, bone marrow, spleen, lung and liver (**Fig. 6f**–**h** and data not shown). Finally, this combination effectively eliminated bone marrow fibrosis (**Fig. 6i**). Together, these results demonstrate that MLN8237 synergizes with ruxolitinib and suggest that combined therapy will show superior activity in patients, as compared to treatment with ruxolitinib alone.

DISCUSSION

In 1984, Castro-Malaspina proposed that ineffective megakaryopoiesis and accumulation of intracytoplasmic components lead to an increase in the levels of a megakaryocyte growth factor (later shown to be platelet-derived growth factor (PDGF)) and a decrease in the levels of platelet factor (PF) 4 within the bone marrow[31]. This combination of elevated PDGF, increased collagen production, reduced PF4 and decreased collagen degradation would then lead to a net increase in collagen and fibrosis. Subsequent studies have documented elevated levels of PDGF, TGF-β and basic fibroblast growth factor (bFGF) in megakaryocytes and platelets of patients with PMF[3,32,33]. More recently, bone morphogenetic proteins (BMPs) and the cytokine oncostatin M have been implicated in myelofibrosis[34,35]. Of these factors, TGF-β produced by megakaryocytes probably has a critical role, as this cytokine is required for the fibrosis that results from increased THPO expression[36].

Whether immature megakaryocytes also drive the other phenotypes in PMF has been less clear. Recipients of *Thpo*-expressing bone marrow progenitors develop a lethal myeloproliferative disorder with fibrosis and other PMF phenotypes, but in this study, expression of the *Thpo* transgene was not restricted to megakaryocytes[14]. Moreover, mice with decreased *Gata1* expression (*Gata1*^{low} mice), which have excessive numbers of immature megakaryocytes in the bone marrow and spleen, develop fibrosis with secondary erythroid defects, but not leukocytosis[16]. These observations suggest that defects in multiple hematopoietic lineages are necessary for PMF pathogenesis. Of note, two elegant recent studies have shown that megakaryocytes influence hematopoietic stem cell (HSC) quiescence[37,38], suggesting that malignant megakaryocytes may have a direct adverse effect on the HSC population. These observations also lend credence to the concept that aberrant megakaryocytes drive the entire spectrum of PMF phenotypes. This model does not preclude contributions to fibrosis from other cell types, such as osteoblastic lineage cells (OBCs), which can be remodeled into inflammatory myelofibrotic cells by exposure to bone marrow cells that express the oncogenic BCR-ABL fusion protein[39]. Although this study[39] implicated Mac1$^+$ myeloid cells in the conversion of OBCs, the role of megakaryocytes in this process was not examined.

AURKA is highly expressed in tumor cells and has been investigated as a therapeutic target in cancer. Indeed, we found that the levels of total and phosphorylated AURKA are greatly elevated in cells that express mutated *CALR*, *MPL*^{W515L} or *JAK2*^{V617F}. Although we cannot formally exclude the possibility that, at least in part, AURKA levels are higher in megakaryocytes from individuals with PMF than in those from normal individuals because PMF megakaryocytes are less mature, the observation that AURKA levels are also elevated in peripheral blood mononuclear cells and purified CD34$^+$ cells from patients with PMF indicates that high levels of AURKA are a common feature of hematopoietic cells in individuals with PMF. Mechanistically, we provide evidence that this phenomenon is mediated by increased expression of c-MYC, which has been shown to be a downstream consequence of activated JAK2 (refs. 25–27). The increase in p-AURKA levels is probably the result of autophosphorylation[40].

© 2015 Nature America, Inc. All rights reserved.

Finally, we discovered that MPN pathogenesis is highly sensitive to AURKA levels, as loss of a single *Aurka* allele led to profound decrease in tumor burden *in vivo* without affecting engraftment or inducing myelosuppression. The lack of myelosuppression observed in these mice, combined with the observation that effective doses of MLN8237 are well tolerated and also do not cause myelosuppression, suggests that a therapeutic window exists for which AURKA inhibition will be effective in treating individuals with PMF, without disrupting normal hematopoiesis.

METHODS

Methods and any associated references are available in the online version of the paper.

Note: Any Supplementary Information and Source Data files are available in the online version of the paper.

ACKNOWLEDGMENTS

We thank A. Stern, J. Licht, Z. Huang and members of the Crispino lab for helpful discussions, and T. Van Dyke (National Cancer Institute) for the generous gift of *Aurka*-floxed mice. We also thank Z. Huang (Wuhan University) for providing the *CALR* T1 and *CALR* T2 plasmids, G. Gilliland (Fred Hutchinson Cancer Research Center) for the *MPL*^{W515L} construct, M. Weiss (St. Jude Children's Research Hospital) for the G1ME cells and T. Arima (Kagoshima University) for the SET-2 cells. This work was supported by US National Institutes of Health (NIH) grant no. HL112792 (J.D.C.), a Leukemia and Lymphoma Society Translational Research Project grant (J.D.C.), the Samuel Waxman Cancer Research Foundation (J.D.C.), a Dixon Young Investigator Award from Northwestern Memorial Foundation (Q.J.W.), the Northwestern University Clinical and Translational Sciences Institute (Q.J.W.) and American Cancer Society grant no. 278808 (Q.J.W.). The project was also supported by the National Center for Research Resources (NCRR), the National Center for Advancing Translational Sciences (NCATS) and the NIH through grant no. TL1R000108 (B.G.).

AUTHOR CONTRIBUTIONS

Q.J.W., Q.Y., B.G., S.M., L.J.B., R.S., L.G. and P.K. performed experiments, interpreted data and contributed to the writing of the manuscript. T.L., A.P., B.S. and A.T. provided patient specimens, interpreted data and contributed to the writing of the manuscript. S.G. and R.K.S. analyzed pathology, interpreted data and contributed to the writing of the manuscript. O.A.-W., A.M., R.L.L. and J.D.C. designed experiments, interpreted data and wrote the manuscript.

COMPETING FINANCIAL INTERESTS

The authors declare no competing financial interests.

Reprints and permissions information is available online at http://www.nature.com/reprints/index.html.

1. Gangat, N. *et al.* DIPSS plus: a refined dynamic international prognostic scoring system for primary myelofibrosis that incorporates prognostic information from karyotype, platelet count and transfusion status. *J. Clin. Oncol.* **29**, 392–397 (2011).
2. Mascarenhas, J. & Hoffman, R. A comprehensive review and analysis of the effect of ruxolitinib therapy on the survival of patients with myelofibrosis. *Blood* **121**, 4832–4837 (2013).
3. Ciurea, S.O. *et al.* Pivotal contributions of megakaryocytes to the biology of idiopathic myelofibrosis. *Blood* **110**, 986–993 (2007).
4. Vannucchi, A.M. *et al.* Mutations and prognosis in primary myelofibrosis. *Leukemia* **27**, 1861–1869 (2013).
5. Abdel-Wahab, O. *et al.* Unraveling the genetic underpinnings of myeloproliferative neoplasms and understanding their effect on disease course and response to therapy: proceedings from the 6th International Post-ASH Symposium. *Am. J. Hematol.* **87**, 562–568 (2012).
6. Tibes, R., Bogenberger, J.M., Benson, K.L. & Mesa, R.A. Current outlook on molecular pathogenesis and treatment of myeloproliferative neoplasms. *Mol. Diagn. Ther.* **16**, 269–283 (2012).
7. Klampfl, T. *et al.* Somatic mutations of calreticulin in myeloproliferative neoplasms. *N. Engl. J. Med.* **369**, 2379–2390 (2013).
8. Nangalia, J. *et al.* Somatic *CALR* mutations in myeloproliferative neoplasms with nonmutated *JAK2*. *N. Engl. J. Med.* **369**, 2391–2405 (2013).
9. Verstovsek, S. *et al.* A double-blind, placebo-controlled trial of ruxolitinib for myelofibrosis. *N. Engl. J. Med.* **366**, 799–807 (2012).
10. Harrison, C. *et al.* JAK inhibition with ruxolitinib versus best available therapy for myelofibrosis. *N. Engl. J. Med.* **366**, 787–798 (2012).
11. Tefferi, A. JAK inhibitors for myeloproliferative neoplasms: clarifying facts from myths. *Blood* **119**, 2721–2730 (2012).
12. Tam, C.S. & Verstovsek, S. Investigational Janus kinase inhibitors. *Expert Opin. Investig. Drugs* **22**, 687–699 (2013).
13. Harrison, C. *et al.* Practical management of patients with myelofibrosis receiving ruxolitinib. *Expert Rev. Hematol.* **6**, 511–523 (2013).
14. Villeval, J.L. *et al.* High thrombopoietin production by hematopoietic cells induces a fatal myeloproliferative syndrome in mice. *Blood* **90**, 4369–4383 (1997).
15. Shivdasani, R.A., Fujiwara, Y., McDevitt, M.A. & Orkin, S.H. A lineage-selective knockout establishes the critical role of transcription factor GATA-1 in megakaryocyte growth and platelet development. *EMBO J.* **16**, 3965–3973 (1997).
16. Vannucchi, A.M. *et al.* Development of myelofibrosis in mice genetically impaired for GATA-1 expression (GATA-1^{low} mice). *Blood* **100**, 1123–1132 (2002).
17. Wen, Q. *et al.* Identification of regulators of polyploidization presents therapeutic targets for treatment of AMKL. *Cell* **150**, 575–589 (2012).
18. Goldenson, B. & Crispino, J.D. The Aurora kinases in cell cycle and leukemia. *Oncogene* **34**, 537–545 (2015).
19. Levine, R.L. *et al.* Activating mutation in the tyrosine kinase JAK2 in polycythemia vera, essential thrombocythemia and myeloid metaplasia with myelofibrosis. *Cancer Cell* **7**, 387–397 (2005).
20. Stachura, D.L., Chou, S.T. & Weiss, M.J. Early block to erythromegakaryocytic development conferred by loss of transcription factor GATA-1. *Blood* **107**, 87–97 (2006).
21. Vannucchi, A.M. *et al.* Abnormalities of GATA-1 in megakaryocytes from patients with idiopathic myelofibrosis. *Am. J. Pathol.* **167**, 849–858 (2005).
22. Uozumi, K. *et al.* Establishment and characterization of a new human megakaryoblastic cell line (SET-2) that spontaneously matures to megakaryocytes and produces platelet-like particles. *Leukemia* **14**, 142–152 (2000).
23. Mullally, A. *et al.* Physiological *Jak2*^{V617F} expression causes a lethal myeloproliferative neoplasm with differential effects on hematopoietic stem and progenitor cells. *Cancer Cell* **17**, 584–596 (2010).
24. Goldenson, B., Kirsammer, G., Stankiewicz, M.J., Wen, Q.J. & Crispino, J.D. Aurora kinase A is required for hematopoiesis but is dispensable for mouse megakaryocyte endomitosis and differentiation. *Blood* **125**, 2141–2150 (2015).
25. den Hollander, J. *et al.* Aurora kinases A and B are upregulated by Myc and are essential for maintenance of the malignant state. *Blood* **116**, 1498–1505 (2010).
26. Wernig, G. *et al.* The *Jak2*^{V617F} oncogene associated with myeloproliferative diseases requires a functional FERM domain for transformation and for expression of the *Myc* and *Pim* proto-oncogenes. *Blood* **111**, 3751–3759 (2008).
27. Sumi, K., Tago, K., Kasahara, T. & Funakoshi-Tago, M. Aurora kinase A critically contributes to the resistance to anticancer drug cisplatin in JAK2V617F mutant–induced transformed cells. *FEBS Lett.* **585**, 1884–1890 (2011).
28. Koppikar, P. *et al.* Efficacy of the JAK2 inhibitor INCB16562 in a mouse model of MPLW515L-induced thrombocytosis and myelofibrosis. *Blood* **115**, 2919–2927 (2010).
29. Wernig, G. *et al.* Efficacy of TG101348, a selective JAK2 inhibitor, in treatment of a mouse model of JAK2V617F-induced polycythemia vera. *Cancer Cell* **13**, 311–320 (2008).
30. Cowley, D.O. *et al.* Aurora A kinase is essential for bipolar spindle formation and early development. *Mol. Cell. Biol.* **29**, 1059–1071 (2009).
31. Castro-Malaspina, H. Pathogenesis of myelofibrosis: role of ineffective megakaryopoiesis and megakaryocyte components. *Prog. Clin. Biol. Res.* **154**, 427–454 (1984).
32. Le Bousse-Kerdilès, M.C. & Martyre, M. C. & French INSERM Research Network on Idiopathic Myeolofibrosis. Involvement of the fibrogenic cytokines, TGF-β and bFGF, in the pathogenesis of idiopathic myelofibrosis. *Pathol. Biol. (Paris)* **49**, 153–157 (2001).
33. Martyré, M.C., Magdelenat, H., Bryckaert, M.C., Laine-Bidron, C. & Calvo, F. Increased intraplatelet levels of platelet-derived growth factor and transforming growth factor-β in patients with myelofibrosis with myeloid metaplasia. *Br. J. Haematol.* **77**, 80–86 (1991).
34. Bock, O. *et al.* Bone morphogenetic proteins are overexpressed in the bone marrow of primary myelofibrosis and are apparently induced by fibrogenic cytokines. *Am. J. Pathol.* **172**, 951–960 (2008).
35. Hoermann, G. *et al.* Identification of oncostatin M as a JAK2V617F-dependent amplifier of cytokine production and bone marrow remodeling in myeloproliferative neoplasms. *FASEB J.* **26**, 894–906 (2012).
36. Chagraoui, H. *et al.* Prominent role of TGF-β1 in thrombopoietin-induced myelofibrosis in mice. *Blood* **100**, 3495–3503 (2002).
37. Bruns, I. *et al.* Megakaryocytes regulate hematopoietic stem cell quiescence through CXCL4 secretion. *Nat. Med.* **20**, 1315–1320 (2014).
38. Zhao, M.P.J. *et al.* Megakaryocytes maintain homeostatic quiescence and promote post-injury regeneration of hematopoietic stem cells. *Nat. Med.* **20**, 1321–1326 (2014).
39. Schepers, K. *et al.* Myeloproliferative neoplasia remodels the endosteal bone marrow niche into a self-reinforcing leukemic niche. *Cell Stem Cell* **13**, 285–299 (2013).
40. Dodson, C.A., Yeoh, S., Haq, T. & Bayliss, R. A kinetic test characterizes kinase intramolecular and intermolecular autophosphorylation mechanisms. *Sci. Signal.* **6**, ra54 (2013).

© 2015 Nature America, Inc. All rights reserved.

ONLINE METHODS

Compounds and plasmids. MLN8237 and diMF were prepared and characterized by ^{1}H NMR (and optical rotation for diMF) at the Broad Institute, as previously reported[17]. Ruxolitinib was purchased from EMD Chemicals. MK-2206 was purchased from Selleck Chemicals. The MSCV-IRES-GFP (Migr1) vector was used to create the Migr1-GFP–MPLW515L, Migr1-GFP–JAK2V617F, Migr1-GFP–CALR-T1 and Migr1-GFP–CALR-T2 plasmids by subcloning the respective genes into the vector, and these constructs were validated by sequencing. Glycerol stocks of empty pLKO.1 and the pLKO.1 c-Myc shRNAs (TRCN0000039640 (sh40) and TRCN0000039642 (sh42)) were purchased from Sigma-Aldrich.

Cell culture. Human HEL cells (obtained from the American Type Culture Collection (ATCC)) were grown in RPMI 1640 medium supplemented with 10% FBS and antibiotics (100 mg/ml penicillin-streptomycin mix) (Thermo Fisher Scientific). Human SET-2 cells[22] were grown in RPMI 1640 medium supplemented with 20% FBS and antibiotics (100 mg/ml penicillin-streptomycin mix) (Thermo Fisher Scientific). G1ME cells were grown in minimal essential medium (MEM)-α (Thermo Fisher Scientific) supplemented with 20% FBS and 1% THPO-conditioned medium, as described previously[20]. For mouse primary bone marrow cell cultures, progenitor cells were enriched from bone marrow of untreated mice either by lineage-negative (Lin$^-$) selection using a progenitor cell enrichment kit (Stemcell Technologies) or by c-Kit–positive selection using a kit from Miltenyi Biotec. Mouse bone marrow progenitor cells were cultured in StemSpan (Stemcell Technologies) supplemented with 10 ng/ml mouse interleukin (IL) 3 (PeproTech), 10 ng/ml human IL-6 (PeproTech) and 40 ng/ml mouse stem cell factor (PeproTech), along with human low density lipoprotein (Stemcell Technologies) (20 μg/ml). To derive megakaryocytes, lineage-depleted mouse bone marrow cells were cultured in the presence of THPO (20 ng/ml; PeproTech) in RPMI 1640 medium supplemented with 10% FBS and antibiotics (100 mg/ml penicillin-streptomycin mix) for various periods of time. Human mononuclear cells were separated from peripheral blood of patients with PMF, ET or PV using Ficoll-Paque PLUS (GE HealthCare Life Sciences) according to the manufacturer's instructions. Human CD34$^+$ cells were purified from peripheral blood mononuclear cells of patients with PMF using a kit from Miltenyi Biotec. CD34$^+$ cord blood and peripheral blood mononuclear cells from healthy donors were purchased from Stemcell Technologies. Human CD34$^+$ cells were cultured in StemSpan medium (Stemcell Technologies) in the presence of recombinant 10 ng/ml human THPO and human SCF (10 ng/ml). Cultured cells were maintained in a humidified atmosphere at 37 °C with 5% CO_2. Cell lines were tested and determined to be mycoplasma free.

Viral transduction. For transfection with retroviruses, plat-E cells (5×10^6) (Cell BioLabs, Inc) were seeded in a 10-cm dish the day before transfection and then transfected with Migr1 plasmids (MSCV-IRES-GFP) containing human *MPL*^{W1515L} or human calreticulin type 1 (*CALR* T1) or type 2 (*CALR* T2) mutations using Fugene VI (Roche), according to the manufacturer's protocols. Forty-eight hours after transfection, the viral supernatant was collected, and 2 ml of viral supernatant was mixed with 5×10^6 mouse bone marrow progenitor cells or G1ME cells in the presence of 8 μg/ml polybrene and 10 mM HEPES (Thermo Fisher Scientific), and then centrifuged at 2,500 r.p.m. for 90 min at 32 °C. Spinoculation was performed twice on the second day after the extraction of the bone marrow cells. For transfection with lentiviruses, 293T cells (5×10^6) (ATCC) were seeded in a 10-cm dish the day before transfection and then transfected with either empty pLKO.1 vector or one with two different shRNAs specific for *MYC* using Fugene VI (Roche). Forty-eight hours after transfection, the viral supernatant was collected, 2 ml of viral supernatant was mixed with 5×10^6 SET-2 cells in the presence of 8 μg/ml polybrene and 10 mM HEPES, and the cells were centrifuged at 2,500 r.p.m. for 90 min at 32 °C. Spinoculation was performed twice on the same day.

***In vitro* inhibitor assays.** Cell lines were plated in 12-well, treated tissue culture plates in 2 ml of medium with DMSO or chemical inhibitors for various periods of time. At the end of the incubation, cell viability was assessed using trypan blue staining (Sigma-Aldrich) or the CellTiter proliferation assay (Promega). Results were normalized to growth of cells in medium containing an equivalent volume of DMSO. The effective concentration at which 50% inhibition in proliferation occurred (IC_{50}) was determined using GraphPad Prism 5.0 software. Primary mouse bone marrow cells were incubated with DMSO or chemical inhibitors in the presence of 10 ng/ml mouse THPO after retroviral transduction. At the end of the incubation, cell surface markers, DNA content and annexin V staining were evaluated by flow cytometry.

Colony-forming unit assays. Assays of colony-forming unit–megakaryocyte (CFU-MK) and colony-forming unit–myeloid (CFU-myeloid) cells were performed on mouse lineage-negative cells. For the CFU-MK assay, 5,000 bone marrow lineage-negative cells were seeded in MegaCult-C medium (Stemcell Technologies) supplemented with 10 ng/ml mouse IL-3 (PeproTech), 10 ng/ml human IL-6 (PeproTech) and 50 ng/ml of mouse THPO (PeproTech), and cultured in the presence of DMSO or chemical inhibitors for 7–9 d. For the CFU-myeloid assay, 2,000 bone marrow lineage-negative cells were seeded in MethoCult medium (Stemcell Technologies) supplemented with 10 ng/ml mouse IL-3 (PeproTech), 10 ng/ml human IL-6 (PeproTech), 10 ng/ml mouse SCF (PeproTech) and 10 ng/ml of mouse granulocyte-monocyte colony stimulating factor (PeproTech), and cultured in the presence of DMSO or chemical inhibitors for 7 d. Slides with MegaCult-grown cultures were fixed with acetone and were then stained with substrates of acetylcholinesterase according to the manufacturer's instructions. Only stained colonies were counted. For the CFU-myeloid assay, colony-forming unit–granulocyte (CFU-G), colony-forming unit–macrophage (CFU-M) and colony-forming unit–granulocyte-macrophage (CFU-GM) colonies were enumerated on day 7 according to the manufacturer's instructions. The number of CFU-myeloid colonies was taken as the sum of CFU-G, CFU-M and CFU-GM colonies.

Synergy studies. Bone marrow cells from C57BL/6 mice (The Jackson Laboratory) were extracted and enriched for c-Kit$^+$ cells. Bone marrow cells were transduced with Migr1 constructs containing human *MPL*^{W1515L} and transplanted into lethally irradiated animals. Three weeks later, mouse bone marrow cells were harvested and plated into MethoCult medium (Stemcell Technologies) with cytokines in the presence of DMSO, MLN8237 or ruxolitinib. The myeloid colonies were enumerated 7 d later and expressed as a fraction of samples that were treated with DMSO. Dose-response curves were generated in GraphPad Prism software. Combination indices were determined using the median-effect principle of Chou and Talalay (CalcuSyn Software)[41].

Animal experiments. *Aurka*-floxed mice on the C57BL/6 background[30] were crossed to *Mx1-Cre* mice[42] (The Jackson Laboratory) to generate *Aurka*$^{fl/+}$*Mx1-Cre* and *Aurka*$^{fl/fl}$*Mx1-Cre* mice. *Jak2*^{V617F} knock-in mice on the C57BL/6 background have been described previously[23]. For the *MPL*^{W515L} model, BALB/c bone marrow progenitor cells were enriched by c-Kit–positive selection and cultured overnight. The next day, the cells were transduced with a retrovirus containing human *MPL*^{W515L}. On the third day, recipient BALB/c mice (The Jackson Laboratory) that had been lethally irradiated with two doses of 550 rad within 24 h were transplanted with the transduced bone marrow cells, and were then transplanted with 3×10^5 GFP$^+$ cells. Recipient mice developed leukocytosis, polycythemia and thrombocytosis in 2–3 weeks. For transplantation of *Jak2*^{V617F}-expressing cells, bone marrow cells from *Jak2*^{V617F} knock-in mice with *Vav-Cre*-mediated expression of Cre recombinase[43] (The Jackson Laboratory) were extracted and a total of 1×10^6 cells were transplanted into irradiated recipient animals. In the drug studies, mice were randomized to treatment groups based on the level of GFP$^+$ tumor cells in the peripheral blood. Vehicle, MLN8237 or diMF was administered to the transplant recipients of the *MPL*^{W515L}- or *Jak2*^{V617F}-expressing cells by oral gavage twice a day, 5 d a week. In these drug studies, the experimental design was such that the researcher assessing the outcome was blinded to the identity of the treatment groups. For the genetic study, three doses of pIpC (GE HealthCare) at 20 mg/kg were given to *Aurka*$^{fl/+}$, *Aurka*$^{fl/+}$*Mx1-Cre*, *Aurka*$^{fl/fl}$ and *Aurka*$^{fl/fl}$*Mx1-Cre* mice on every other day by intraperitoneal (i.p.) injection. All experiments were conducted in accordance with animal protocols approved by the Northwestern University Institutional Animal Care and Use Committee. Group sizes were determined by performing a power calculation to lead to a 90% chance of detecting a significant difference ($P < 0.05$) in the megakaryocytic tumor burden across

© 2015 Nature America, Inc. All rights reserved.

the treatment groups. Female mice between 8 and 12 weeks of age were used for all transplantation studies.

Complete blood counts. Blood (50 μl) was collected from the tail vein in EDTA-coated tubes and analyzed by a Hemavet 850 complete blood counter (Drew Scientific).

Flow cytometry. Bone marrow cells were flushed from hind leg bones with PBS (Gibco) + 2% FBS + penicillin-streptomycin (Cambrex). Spleen cells were prepared by pressing tissue through a cell strainer. In both cases, cells were lysed on ice with red blood cell lysis solution (Puregene lysis solution; Qiagen). Single-cell suspensions of bone marrow, spleen or cell lines were prepared by resuspending the cells in PBS with 0.5% BSA (Sigma) and 2 mM EDTA (Gibco). Surface marker staining using antibodies for human or mouse CD41 (GPIIb; BD Bioscience 561850 (mouse) and 555469 (human), San Diego, CA) and CD42b (GPIb; BD Bioscience 551061 (human) or Emfret Analytics M040-3 (mouse), Wurzburg, Germany) was performed by incubation for 30 min in Ca^{2+}-free, Mg^{2+}-free PBS. Staining for the following mouse surface makers was done in a similar manner using the antibodies mentioned: Ter119 (BD Bioscience 0560504), CD71 (BD Bioscience 555535), Gr-1 (BD Bioscience 553129) and Mac1 (BD Bioscience 555388). Mouse bone marrow cells were also stained using a mouse hematopoietic progenitor enrichment kit (Stemcell Technologies 19756) that contained antibodies to CD5, CD11b, CD19, CD45R, Gr-1 and TER119; enrichment was followed by staining with Pacific blue–labeled streptavidin. Cells were simultaneously stained with antibodies against c-Kit (eBioscience 17-1171), Sca-1 (eBioscience 25-5981), CD34 (eBioscience, 13-0341) and Fc-γR (eBioscience 45-0161) to label stem and myeloid progenitor populations, including LSK, CMP, GMP and MEP cells, as previously described[44]. For annexin V staining, cells were incubated with an annexin V antibody (BioVision, K103-25) in staining buffer (10 mM HEPES, 140 mM NaCl, 2.5 mM $CaCl_2$, pH 7.4) for 15 min. For DAPI staining, mouse or human cells were fixed in 2% paraformaldehyde at room temperature for 10 min and stained with a 4,6-diamidino-2-phenylindole (DAPI; Sigma) and saponin solution, containing 0.1% saponin and 1 μg/ml DAPI, to determine DNA content. DNA content, surface marker expression, myeloid progenitor staining and apoptosis were determined using a LSR II flow cytometer (BD Biosciences). Data were analyzed using FlowJo software (Treestar, Ashland, OR). In the experiment in which mouse lineage-depleted bone marrow cells were differentiated to megakaryocytes, cells were stained with the anti-CD41 antibody and sorted using a FACSAria instrument (BD Biosciences, Mountain View, CA).

PCR analysis. Genomic DNA was extracted from mouse bone marrow, spleen and peripheral blood cells using a kit from Qiagen. To detect the WT and floxed *Aurka* alleles, forward (5′-CCTGTGAGTTGGAAAGGGACATGGCTG-3′) and reverse (5′-CCACCACGAAGGCAGTGTTCAATCCTAAA-3′) primers were used to amplify the 500-bp and 600-bp PCR products, respectively. To detect the excision of the floxed *Aurka* allele, forward (5′-CAGAG TCTAAGTCGAGATATCACC TGAGGGTTGA-3′) and reverse (5′-GATGGAAA CCCTGAGCACCTGTGAAAC-3′) primers were used to amplify a 300-bp PCR product. To detect the *Mx1-Cre* transgene, forward (5′-GCCTGCATTAC CGGTCGATGCAACGA-3′) and reverse (5′-GTGGCAGATGGCGCGGCAA CACCAT-3′) primers were used to amplify a 600-bp PCR product.

Western blots. Cells were lysed in RIPA buffer (Tris-HCl, 50 mM, pH 7.4; NP-40, 1%; sodium deoxycholate, 0.25%; NaCl, 150 mM; EDTA, 1 mM) supplemented with protease inhibitors (pepstatin, leupeptin and aprotinin, each at 10 μg/ml; PMSF, 1 mM) and phosphatase inhibitor (Na_3VO_4, 1 mM). Proteins were separated by SDS-PAGE and transferred to a PVDF membrane. Membranes were blotted with antibodies detecting p-AURKA (Cell Signaling 2914), p-STAT3 (Cell Signaling 9145), p-STAT5 (Cell Signaling 9359), STAT3 (Cell Signaling 4904), STAT5 (Cell Signaling 9363), AURKA (GeneTex GTX13824), GRB2 (BD Bioscience 610111) and HSC70 (Santa Cruz Biotechnology SC7298).

Histopathology. Tissues were fixed in 10% neutral-buffered formalin, embedded in paraffin, and stained with hematoxylin and eosin or with reticulin to assess for fibrosis. Blood smears were fixed in methanol and stained in Giemsa and May-Grunwald solutions. Images of histological slides were obtained on a Leica DM4000B microscope (Leica) equipped with a Leica DFC320 color digital camera (Leica).

Patient samples. Primary specimens from patients with PMF, ET or PV were obtained after informed consent in accordance with protocols approved by the Northwestern University and the Mayo Clinic Institutional Review Boards. Details on each patient are provided in **Supplementary Tables 1** and **2**. $CD34^+$ cells from umbilical cord blood and mononuclear cells, both from healthy individuals, were purchased from Stemcell Technologies.

Statistical analyses. For quantitative assays, treatment groups were reported as mean ± s.d. and compared using the unpaired two-sided Student's *t*-test. When multiple comparisons were necessary, one-way or two-way analysis of variance (ANOVA) with post hoc Bonferroni correction was used. Statistical significance was established at $P < 0.05$, and labeled as $^*P < 0.05$ and $^{**}P < 0.01$. All analysis was performed using GraphPad Prism version 4.01 for Windows (GraphPad Software).

41. Chou, T.C. & Talalay, P. Quantitative analysis of dose-effect relationships: the combined effects of multiple drugs or enzyme inhibitors. *Adv. Enzyme Regul.* **22**, 27–55 (1984).
42. Kühn, R., Schwenk, F., Aguet, M. & Rajewsky, K. Inducible gene targeting in mice. *Science* **269**, 1427–1429 (1995).
43. de Boer, J. *et al.* Transgenic mice with hematopoietic and lymphoid specific expression of *Cre*. *Eur. J. Immunol.* **33**, 314–325 (2003).
44. Akashi, K., Traver, D., Miyamoto, T. & Weissman, I.L. A clonogenic common myeloid progenitor that gives rise to all myeloid lineages. *Nature* **404**, 193–197 (2000).

© 2015 Nature America, Inc. All rights reserved.

doi:10.1038/nm.3995